Journal of Intelligent Systems and Internet of Things
Vol. 12, No. 01, PP. 33-44, 2024
DOI: https://doi.org/10.54216/JISIoT.120103

Enhancing Brain Tumor Detection and Classification using Osprey Optimization Algorithm with Deep Learning on MRI Images

S. Stephe[1,*], V. Nivedita[2], B. Karthikeyan[3], K. Nithya[4], Mohamed Yacin Sikkandar[5]

[1]Department of Electronics and Communication Engineering, K. Ramakrishnan College of Engineering, Tiruchirapalli, India;
[2]Department of Computer Science and Engineering, SRMIST Ramapuram Campus, Chennai- 89, India;
[3]Department of Information Technology, Panimalar Engineering College, Chennai;
[4]Department of Computer Science and Engineering, School of Computing, Vel Tech Rangarajan Dr.Sagunthala R&D Institute of Science and Technology, Chennai, India;
[5]Department of Medical Equipment Technology, College of Applied Medical Sciences, Majmaah University, Al Majmaah 11952, Saudi Arabia
Emails: stephes.ece@krce.ac.in; niveditv1@srmist.edu.in; karthikeyan.b32@gmail.com; nithyakmaha@gmail.com; m.sikkandar@mu.edu.sa
[*]Corresponding Author: stephes.ece@krce.ac.in

Abstract

Brain tumors (BT) are abnormal cell growth from the brain or the surrounding cells. It is categorized into 2 major types such as malignant (cancerous) and benign (non-cancerous). Classifying and detecting BTs is critical for knowledge of their mechanisms. Magnetic Resonance Imaging (MRI) is a helpful but time-consuming system, that needs knowledge for manual examination. A new development in Computer-assisted Diagnosis (CAD) and deep learning (DL) allows more reliable BT detection. Typical machine learning (ML) depends on handcrafted features, but DL achieves correct outcomes without such manual extraction. DL methods, particularly convolutional neural networks (CNNs) and recurrent neural networks (RNNs) can exposed to optimum outcomes in the domain of medical image analysis, comprising the classification and recognition of BTs in MRI and CT scans. Thus, the study designs an automated BT Detection and Classification using the Osprey Optimization Algorithm with Deep Learning (BTDC-OOADL) method on MRI Images. The BTDC-OOADL technique deeply investigates the MRI for the identification of BT. In the proposed BTDC-OOADL algorithm, the Wiener filtering (WF) model is applied for the elimination of noise. Besides, the BTDC-OOADL algorithm exploits the MobileNetV2 technique for the procedure of feature extractor. In the meantime, the OOA is utilized for the optimum hyperparameter choice of the MobileNetv2 model. Finally, the graph convolutional network (GCN) model can be deployed for the classification and recognition of BT. The experimental outcome of the BTDC-OOADL methodology can be tested under benchmark dataset. The simulation values infer the betterment of the BTDC-OOADL system with recent approaches.

Received: January 30, 2023 Revised: February 18, 2023 Accepted: March 28, 2024

Keywords: Brain tumor; Computer-aided diagnosis; Osprey optimization algorithm; deep learning; Brain MRI

1. Introduction:

Nowadays, brain tumor (BT) is the most dangerous disease that affects the human body. Cancers are commonly detected in numerous regions of the brain [1]. It can lead to difficulty with body functions when there are some cancers in the brain, which are simply diagnosed cancers employing some image processing methods or via a manual segmentation technique [2]. Diagnosing malignant tumors in various regions of the body and performing rapidly to

treat them is complicated. According to new research, the common occurrence of BT could be drastically increased [3]. It could be only later that the indications of these cancers become evident, posing an important risk to human beings. All signs of a brain disorder namely vision loss, frequent headaches, Speech or hearing problems, memory loss, and personality variations. Magnetic resonance imaging (MRI) is a major popular technology to detect BT [4]. It is an extensively utilized non-intrusive imaging pattern that provides sensitive difference among tissues. Imaging configurations of importance in human BT could be assisted by the proficiency of MRI to provide tissues, which is frequently regularized [5]. Research workers have recently been challenged with a problem and difficult concerns regarding manually segmenting brain MRI [6].

Numerous techniques for computer-aided diagnoses (CAD) were introduced for automatically analyzing BT [7]. Recently, amongst several other applications, artificial intelligence (AI) has represented optimistic outcomes as a decision support system (DSS) to support the Identification of diseases and the establishment of detailed medical analyses [8]. Various research workers examined abundant methods to diagnose and classify BT with lesser error and better performance. Deep Learning (DL) approaches are broadly exploited to make an automatic technique that can precisely segment or classify BT in the shortest time [9]. DL allows the application of a pre-trained CNN method for medical images, particularly for the classification of B which is made for different applications such as ResNet-34, GoogLeNet, and AlexNet. DL is composed of a multi-layered deep neural network (DNN) [10]. The backpropagation (BP) approach has been utilized by a neural network (NN) to decrease the error among the actual and target values. While the number of layers improves, designing an ANN framework is highly complex.

This study designs an automatic BT Detection and Classification using the Osprey Optimization Algorithm with DL (BTDC-OOADL) algorithm on MRI. The BTDC-OOADL technique deeply investigates the MRI for the identification of BT. In the proposed BTDC-OOADL method, the Wiener filtering (WF) method is used for the noise removal. Besides, the BTDC-OOADL approach exploits the MobileNetv2 technique for the procedure of feature extractor. In the meantime, the OOA is deployed for the boost parameter selection of the MobileNetv2 algorithm. Finally, the graph convolutional network (GCN) model is utilized for the classification and detection of BT. The experimental value of BTDC-OOADL method can be tested on benchmark datasets.

2. Literature Review

The authors [11] established an automated method for BT classification and identification employing a saliency map and DL feature optimizer. Primarily, a fusion-based contrast enhancement approach has been implemented. Secondarily, a cancer segmentation algorithm that depends on saliency maps has been developed. Lastly, the better features can be categorized by utilizing an extreme learning machine (ELM). Vankdothu and Hameed [12] introduced a new automated method for identification and classification. Image segmentation has been executed utilizing the improved K-means clustering (IKMC) method, and the GLCM has been applied for extracting features for removing features. The classification technique was accomplished by utilizing recurrent-CNNs (RCNNs). In [13], an approach that depends on deep-CNNs (DCNNs) employing MRI data was introduced. Conditional random fields (CRF) for removing counterfeit outputs, regarding spatial data on reasonable segmentation tasks. The primary developed model categorizes BT. A secondary model distinguishes between low- and high-grade gliomas (LGG and HGG, correspondingly).

The authors [14] presented a new Multi-objective AOA with the Fusion-based DL (MOAOA-FDL) method. The ant colony optimization (ACO) with Shannon entropy-based multi-level thresholding method was established segmentation. Similarly, the fusion of 2 DL algorithms such as EfficientNet and MobileNet architecture, could be utilized for extracting feature techniques. Lastly, the AOA with LSTM technique was implemented for the classification method. Mandle et al. [15] employed a VGG-19 CNNs-based DL approach. Firstly, the contrast enhancement method was utilized for removing noises. Secondly, a DNN has been exploited for extraction. Aziz et al. [16] designed an architecture employing an ensemble of optimum DL features. Primarily, a database is normalized followed by 2 pre-trained DL algorithms that have been selected such as ResNet50 and Densenet201. The enriched ACO method was implemented for efficient feature selection (FS) from deep methods. The chosen features were incorporated employing a serial-based technique and categorized by a cubic SVM.

In [17], an architecture dependent upon CNNs with Mass Correlation Analysis (MCA) was introduced. Now, the input database has been primarily engaged in preprocessing where the Average Mass Elimination Algorithm (AMEA) could be implemented. The important features are obtained employing Median values of white mass. Afterwards, the removed features have been trained by CNN technique depending on MCA that supports to allocation of the weight

measure. Raza et al. [18] developed a hybrid DL method named DeepTumorNet by exploiting a main CNN model. In the DeepTumorNet technique, the final 5 layers of GoogLeNet are extracted, and 15 new layers are included rather than these 5 layers.

3. The Proposed Model

In this manuscript, we have designed a new BTDC-OOADL for accurate recognition and classification of the BT on MRI Images. The BTDC-OOADL technique deeply investigates the MRI for the BT diagnosis. In the proposed BTDC-OOADL method, several subprocesses are included namely WF-based noise removal, MobileNetv2 feature extractor, OOA-based parameter tuning, and GCN-based classification. Fig. 1 illustrates the entire procedure of the BTDC-OOADL technique.

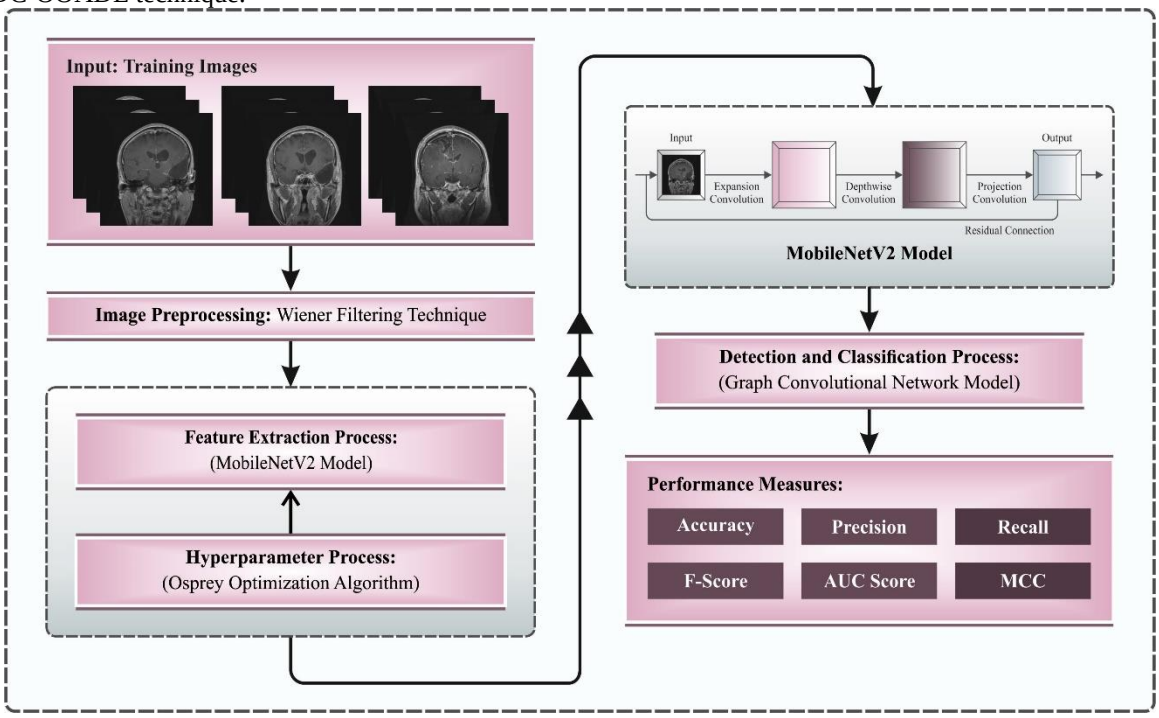

Figure 1: Overall process of BTDC-OOADL algorithm

A. WF-based Noise Removal

Primarily, the WF model is exploited for eliminating the noise in the brain MRI. The WF is a beneficial image processing system deployed in terms of brain MRI to improve image quality and decrease noise [19]. By deploying statistical data on the noise and signal features, the WF efficiently suppresses unwanted noise while maintaining essential structural details in MRI images. This adaptive filter system can be particularly valuable for enhancing the clarity and diagnostic accuracy of brain MRI scans, supporting medical staff in optimum exploring, and interpreting the images for the analysis and treatment of neurological states.

B. Feature Extraction

The MobileNetv2 model is applied for the process of feature extraction. The presented model utilizes MobileNetV2 as the base model [20]. MobileNetV2 has been established in MobileNetV1 by integrating inverted remaining with linear bottleneck components. MobileNet structure depends on depthwise separable convolutional. The archetypal 2D convolutional procedures every input channel straight to generate one channel by convolving from the depth size (channel) equally. The depthwise convolutional divides the input images and the filtered into various channels followed by integrating all the input channels with equivalent filtered channels. Then the filtered resultant channel is created, and individual resultant channels can stack back. During the depthwise separable convolution, the stacked resultant channels are after filter utilizing an 11 convolutional named pointwise convolutional, for combining the stacked resultant channels into 1 channel. The depthwise convolutional generates a similar outcome as the typical convolutional; however, it is more effectual as it decreases the parameter counts contained in the procedure. By calculating the pointwise and depthwise convolutional as divided layers, MobileNetV1 takes 28 convolution layers that create an outcome with dimensional 771280 pixels.

Either MobileNetV1 or MobileNetV2 get input images with dimensional of 2242243 pixels. Thus, the input images on the database can be cropped and resized into 224224 pixels. MobileNetV2 inserts 19 inverted remaining bottleneck

layers and then the 1st convolutional layer with 32 filters after ending with pointwise convolutional to generate an outcome with dimensional 771280 pixels. The remaining block links the start and termination of the convolution block with skip connection with the drivers of carrying data to the deep layer of networks. During the typical remaining block, the start and termination of the convolution block generally are additional channels than the layers.

C. OOA-based Hyperparameter Tuning

At this phase, the OOA is executed for the hyperparameter choice of the MobileNetv2 algorithm. The Osprey generally called the sea hawk, fish, and river, is a nocturnal fish-eating bird of prey with an extensive geographic region [21]. Based on the osprey behaviours, the position updating process of osprey in the two stages of exploration and exploitation is presented after the initiation of OOA and is discussed below.

OOA is a population-based technique that employs a repetition-based approach and searches for the best possible solution depending on the search capability of the population member. All the ospreys evaluate the value of the problem variable as a population member based on location. Consequently, the osprey signifies a possible outcome to the problems, defined as a vector. The osprey location can be randomly initialized in the search space.

$$X = \begin{bmatrix} X_1 \\ \vdots \\ X_i \\ \vdots \\ X_N \end{bmatrix}_{N\times m} = \begin{bmatrix} x_{1,1} & \cdots & x_{1,j} & \cdots & x_{1,m} \\ \vdots & \ddots & \vdots & \ddots & \vdots \\ x_{i,1} & \cdots & x_{i,j} & \cdots & x_{i,m} \\ \vdots & \therefore & \vdots & \ddots & \vdots \\ x_{N,1} & \cdots & x_{N,j} & \cdots & x_{i,m} \end{bmatrix}_{N\times m} \quad (1)$$

$$x_{i,j} = lb_j + r_{i,j} \cdot \left(ub_j - lb_j\right), i = 1,2,\dots,N, j = 1,2,\dots,m, \quad (2)$$

Now the population matrix of osprey location is X, the j^{th} ospreys (a candidate solution) is X_i s, $x_{i,j}$ denotes the j^{th} dimension, the amount of ospreys is N, the number of problem variables is m, random integers within $[0,1]$ is $r_{i,j}$, the low and up boundaries of the search space are lb_j and ub_j.

The objective function is evaluated meanwhile every individual osprey is a possible outcome to the problems that correspond to that specific osprey. Based on Eq. (3), a vector represents the value evaluated for the objective function of the problems.

$$F = \begin{bmatrix} F_1 \\ \vdots \\ F_{\mathrm{i}} \\ \vdots \\ F_{\mathrm{N}} \end{bmatrix}_{N\times 1} = \begin{bmatrix} F(X_1) \\ \vdots \\ F(X_{\mathrm{i}}) \\ \vdots \\ F(X_{\mathrm{N}}) \end{bmatrix}_{N\times 1} \quad (3)$$

In Eq. (3), the vector of main function values is F and the evaluated value of the objective function for i^{th} ospreys is F_i.

Phase1: Detection of Positions and Hunting of Fish (Exploration)

The initial phase of OOA's population update was modelled by simulating the osprey behaviours. The osprey location significantly changed by raising the exploration capability of the OOA in finding the best position, escaping the local optima, and modelling the osprey attack on fish. The placement of other ospreys that have high objective function values in the search space was considered as undersea fish for all the ospreys in the OOA. The group of fish for every individual osprey can be defined using Eq. (4):

$$FP_i = \{X_k | k \in \{1,2,\dots,N\} \wedge F_k < F_i\} \cup \{X_{best}\} \quad (4)$$

In Eq. (4), the fish location set for the i^{th} ospreys is FP_i and the optimum osprey solution is X_{best}.

This fish is located randomly by the ospreys which later strike it. Based on Eq. (5), an updated location for the corresponding osprey was defined according to the simulation of osprey's motion near the fish. Based on Eq. (6), the osprey moves toward the newest location if it increases the objective function value.

$$x_{i,j}^{P1} = x_{i,j} + r_{i,j} \cdot \left(SF_{i,j} - I_{i,\mathrm{j}} \cdot x_{i,\mathrm{j}}\right),$$

$$X_{i,j}^{P1=} \begin{cases} x_{i,j}^{P1}, \mathrm{l}b_j \le x_{i,j}^{P1} \le ub_j; \\ \mathrm{l}b_j^{P1}, x_{i,j}^{P1} < \mathrm{l}b_j; \\ \mathrm{u}b_j^{P1}, x_{i,j}^{P1} > \mathrm{u}b_j. \end{cases} \quad (5)$$

$$X_i = \begin{cases} X_i^{P1}, F_i^{P1} < F_i; \\ X_i, \quad else, \end{cases} \quad (6)$$

Here, the new position of i^{th} ospreys based on the initial stage of OOA is X_i^{P1}, $x_{i,j}^{P1}$ refers to the j^{th} dimension, F_i^{P1} indicates the fitness function, the fish nominated for i^{th} osprey is SP_i, the j^{th} dimension is $SP_{i,j}$, random number within $[0,1]$ are $r_{i,j}$, and $I_{i,j}$ are randomly generated integer ranges from 1 to 2.

Phase2: Performing the Fish to the Suitable Location Position (Exploitation)

The osprey carrying the fish has caught to better position, but they consume it. In the OOA, the second phase of upgrading the population was modelled according to the imitation of real behaviours. The osprey's position was generated by slight modification caused by modelling the fish performing to the appropriate location that increases the exploitation ability in the local search and converges towards the best solution closer to the obtained solution. The random location was initially defined in the OOA for population members as a "suitable location for eating fish".

It replaces the previous position if the objective function is improved in this newest location.

$$x_{i,j}^{P2} = x_{i,j} + \frac{\mathrm{l}b_j + r \cdot \left(ub_j - \mathrm{l}b_j\right)}{t}, i = 1,2, \ldots, N, j = 1,2, \ldots, m, t = 1,2, \ldots, T,$$

$$x_{i,j}^{P2=} \begin{cases} x_{i,j}^{P2}, \mathrm{l}b_j \le x_{i,j}^{P2} \le ub_j; \\ \mathrm{l}b_j, x_{i,j}^{P2}, < \mathrm{l}b_j; \\ ub_j, x_{i,j}^{P2} > ub_j, \end{cases} \quad (7)$$

$$X_i = \begin{cases} X_i^{P2}, F_i^{P2} < F_i; \\ X_i, else, \end{cases} \quad (8)$$

Where the i^{th} ospreys' new location dependent upon the second stage of OOA is X_i^{P2}, $x_{i,j}^{P2}$ denotes the j^{th} dimension, F_i^{P2} represents the fitness function (FF), $r_{i,j}$ are arbitrarily generated integers in zero and one, t and T are the iteration and overall amount of iterations.

The fitness selection is a key feature of OOA technique. An encoder performance was utilized for establishing the superior outcome of the candidate result. Here, the accuracy value is an essential condition employed to design an FF.

$$Fitness = \max(P) \quad (9)$$

$$P = \frac{TP}{TP + FP} \quad (10)$$

Whereas FP and TP are the false and true positive values.

D. Image Classification using GCN

The GCN algorithm is utilized for image classification. The model is an NN that works on graphs directly and influences their structural data [22]. The GCN input is a graph $= (V, E)$, where the set of edges and nodes are E and V correspondingly. V is signified as an NxF feature matrix X, collected by the feature vector of distance F connected with N nodes. The structural data of the graph surrounded in E is defined as NxN adjacent matrix A. GCN model produces a node-level outcome O in the method of NxK matrix, whereas the count of resultant features calculated for every node is K.

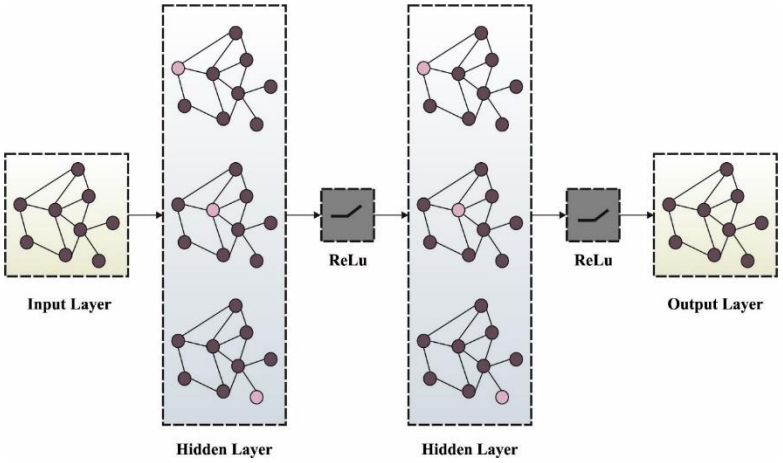

Figure 2: Architecture of GCN

This matrix is expressed as the adjacency matrix A and function of feature matrix X as:

$$O = f(X, A) = \sigma(AXW) \quad (11)$$

Here W is an FxK trainable weighted matrix.

Once multiplied by A, a weighted amount is computed for every node amongst the feature vectors of each adjacent node. Due to this, the self-loop is included by representing $\hat{A} = A + I$, whereas I is an $N \times N$ identity matrix. Then, A is normally not normalized, and the matrix multiplication signified in Eq. (11) causes a scale alteration in the feature vectors. To avoid numerical variabilities and gradient explosion, the adjacent matrix is regularized by evaluating $D^{\frac{1}{2}}AD\ ^{\frac{1}{2}}$, where $D_{ii} = \sum_j A_{ij}$, the diagonal node degree matrix is D. Fig. 2 depicts the architecture of GCN.

By considering the previous changes, the GCN layer output is expressed as:

$$O = f(X, A) = \sigma\left(D^{\frac{1}{2}}\hat{A}D^{\frac{1}{2}}XW\right) \quad (12)$$

It is highly probable to describe a multilayer GCN by providing the resultant feature matrix of the layer composed of adjacent matrix A as input for the subsequent layer. Normally, GCN is tested by reducing loss function $\mathcal{L}$ determined among its outcome O and the predictable outcome $\overline{O}$ through the BP technique.

4. Results and Discussion

The BT recognition outcomes of the BTDC-OOADL approach are tested on the MRI database from the Kaggle repository [23]. The database includes 5500 samples with 4 class labels as defined in Table 1. Fig. 3 depicts the sample images.

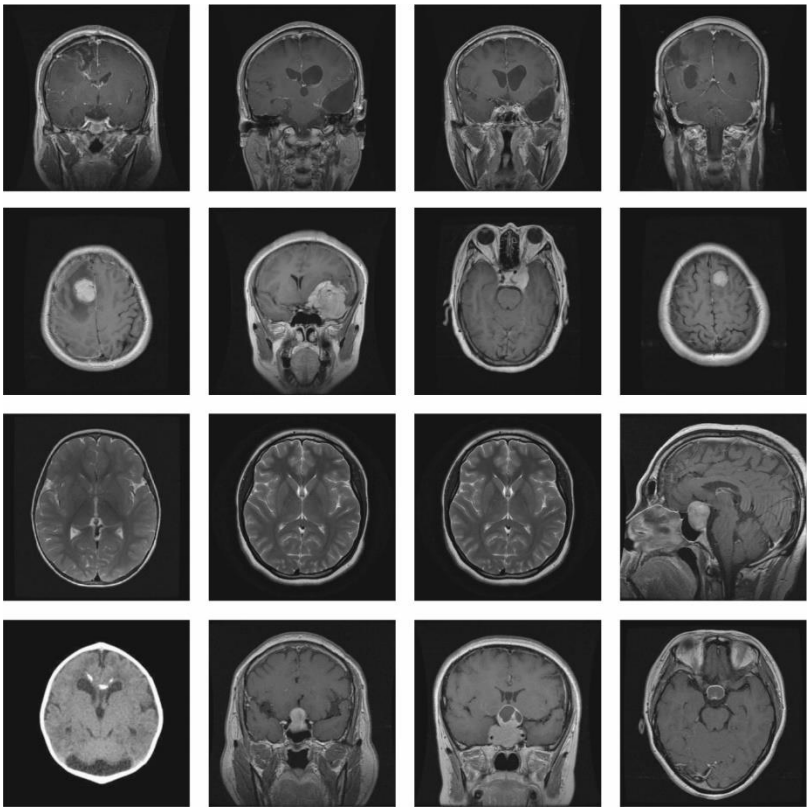

Figure 3: Sample images

The confusion matrices generated by the BTDC-OOADL model under 80%:20% and 70%:30% of the TRAS/TESS is depicted in Fig. 4. The outcomes represent the proficient recognition of four class labels.

The BT recognition outcome of the BTDC-OOADL method is exhibited at 80%:20% of the TRAS/TESS is shown in Table 2 and Fig. 5. The outcome values highlighted that the BTDC-OOADL model obtains better outcomes on four class labels. With 80% of the TRAS, the BTDC-OOADL model provides an average $accu_y$, $prec_n$, $reca_l$, F_{score}, AUC_{score}, and MCC of 99.39%, 98.80%, 98.77%, 98.78%, 99.18%, and 98.37%, correspondingly. Furthermore, based on 20% of the TESS, the BTDC-OOADL method provides an average $accu_y$, $prec_n$, $reca_l$, F_{score}, AUC_{score}, and MCC of 99.36%, 98.73%, 98.72%, 98.72%, 99.14%, and 98.30%, correspondingly

Table 1: Database Details

Classes	No. of Images
Glioma	1300
Meningioma	1300
No-Tumor	1500
Pituitary	1400
Total Images	5500

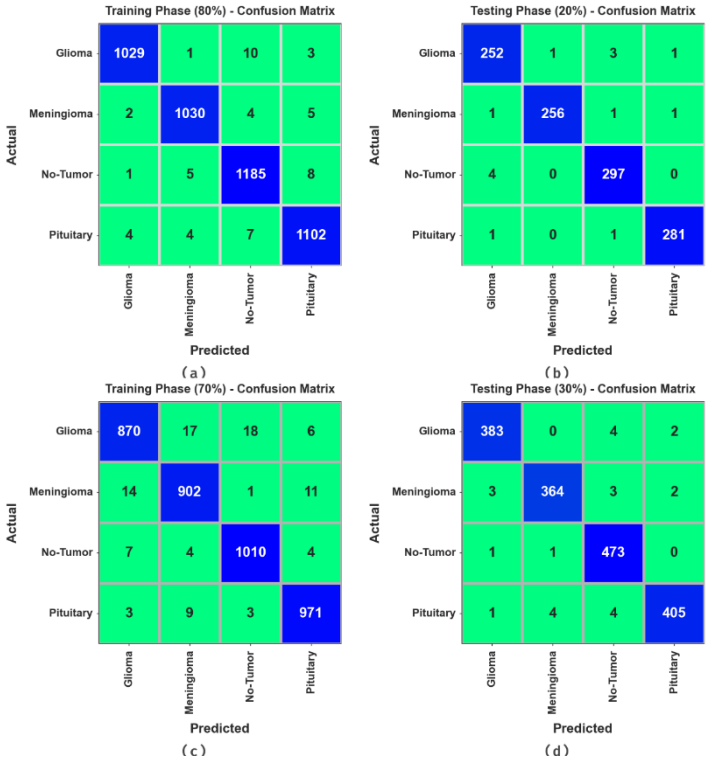

Figure 4: Confusion matrices of (a-c) TRAS of 80% and 70% and (b-d) TESS of 20% and 30%

Table 2: BT outcome of BTDC-OOADL approach with 80%:20% of TRAS/TESS

Classes	$Accu_y$	$Prec_n$	$Reca_l$	F_{score}	AUC_{score}	MCC
TRAS (80%)						
Glioma	99.52	99.32	98.66	98.99	99.22	98.68
Meningioma	99.52	99.04	98.94	98.99	99.32	98.68
No-Tumor	99.20	98.26	98.83	98.54	99.09	98.00
Pituitary	99.30	98.57	98.66	98.61	99.08	98.14
Average	99.39	98.80	98.77	98.78	99.18	98.37
TESS (20%)						
Glioma	99.00	97.67	98.05	97.86	98.67	97.21
Meningioma	99.64	99.61	98.84	99.22	99.36	98.99
No-Tumor	99.18	98.34	98.67	98.51	99.02	97.94
Pituitary	99.64	99.29	99.29	99.29	99.52	99.05
Average	99.36	98.73	98.72	98.72	99.14	98.30

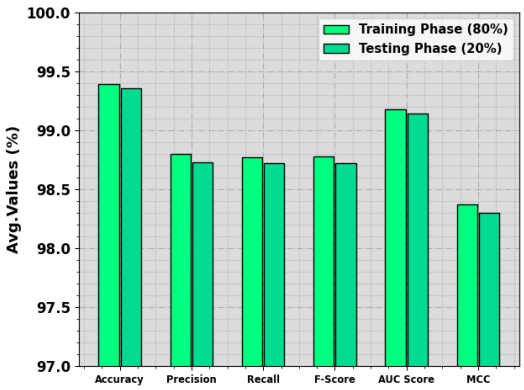

Figure 5: Average of BTDC-OOADL approach with 80%:20% of TRAS/TESS

The BT recognition results of the BTDC-OOADL model at 70%:30% of the TRAS/TESS is shown in Table 3 and Fig. 6. The simulated values show that the BTDC-OOADL model achieves efficient results with all four classes.

Table 3: BT outcome of BTDC-OOADL approach with 70%:30% of TRAS/TESS

Class	$Accu_y$	$Prec_n$	$Reca_l$	F_{score}	AUC_{score}	MCC
TRAS (70%)						
Glioma	98.31	97.32	95.50	96.40	97.34	95.30
Meningioma	98.55	96.78	97.20	96.99	98.09	96.03
No-Tumor	99.04	97.87	98.54	98.20	98.88	97.55
Pituitary	99.06	97.88	98.48	98.18	98.87	97.55
Average	98.74	97.46	97.43	97.44	98.29	96.61
TESS (30%)						
Glioma	99.33	98.71	98.46	98.58	99.03	98.15
Meningioma	99.21	98.64	97.85	98.25	98.73	97.74
No-Tumor	99.21	97.73	99.58	98.64	99.32	98.10
Pituitary	99.21	99.02	97.83	98.42	98.75	97.90
Average	99.24	98.53	98.43	98.47	98.96	97.97

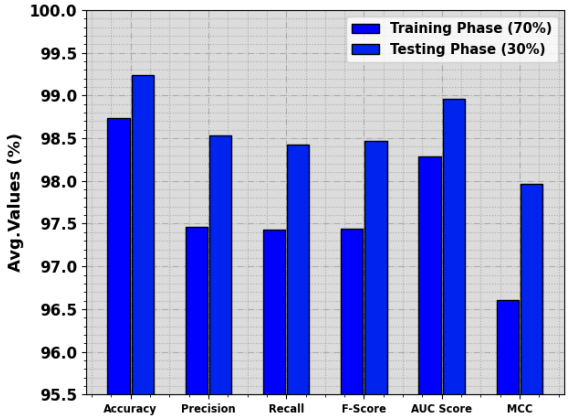

Figure 6: Average of BTDC-OOADL approach with 70%:30% of TRAS/TESS

With 70% of the TRAS, the BTDC-OOADL model provides an average $accu_y$, $prec_n$, $reca_l$, F_{score}, AUC_{score}, and MCC of 98.74%, 97.46%, 97.43%, 97.44%, 98.29%, and 96.61%, correspondingly. In addition, with 30% of the TESS, the BTDC-OOADL method provides an average $accu_y$, $prec_n$, $reca_l$, F_{score}, AUC_{score}, and MCC of 99.24%, 98.53%, 98.43%, 98.47%, 98.96%, and 97.97%, correspondingly.

Figure 7: $Accu_y$ curve of BTDC-OOADL method under 80%:20% of TRAS/TESS

To measure the outcome of the BTDC-OOADL algorithm under 80%:20% of TRAS/TESS, TRA and TES $accu_y$ outcomes are well-defined, as exposed in Fig. 7. The TRA and TES $accu_y$ analysis exhibit the outcomes of the BTDC-OOADL method under several epochs. The outcome provides meaning detailed underlying the learning model and generalized abilities of the BTDC-OOADL model. With a higher count of epochs, it is noted that the both $accu_y$ attains superior outcomes. It can be detected that the BTDC-OOADL system achieves higher testing $accu_y$ that can identify the outlines in both databases.

The overall TRA and TES losses outcomes of the BTDC-OOADL model under 80%:20% of the TRAS/TESS under epochs is shown in Fig. 8. The TRA loss outperforms the loss model obtains minimal with epochs. Generally, the loss outcomes are minimal as the model alters the weight to decrease the predictive outcome on both databases. The loss outcomes depict the level, but the model can appropriate the trained dataset. It can be experimental that the TRA and TES losses can slowly decrease and exhibited that the BTDC-OOADL method effectively gains the designs exposed in both datasets. Note that the BTDC-OOADL method fine-tuned the bounds to lessen the deviation between the original and predictive trained model.

Figure 8: Loss curve of BTDC-OOADL approach at 80%:20% of TRAS/TESS

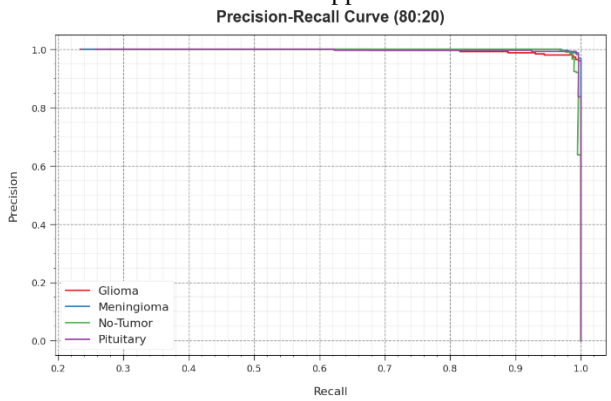

Figure 9: PR curve of BTDC-OOADL method at 80%:20% of TRAS/TESS

The PR outcome of the BTDC-OOADL method on 80%:20% of TRAS/TESS is exhibited by plotting $prec_n$ against $reca_l$ as exposed in Fig. 9. The outcome implied that the BTDC-OOADL method achieves higher PR outcomes under 4 class labels. The simulation value exposed that the method gains for detecting several classes. The BTDC-OOADL algorithm achieves superior outcomes in the recognition of positive instance with least false positives.

The ROC outcomes attained by the BTDC-OOADL method on 80%:20% of TRAS/TESS is exposed in Fig. 10 which is the ability in the discrimination of the classes. The outcomes represent appreciated findings on the trade-offs amongst the FPR and TPR rates under dissimilar classifier thresholds and different epoch counts. It proposes the accurate prediction outcomes of the BTDC-OOADL method on the classifying of different class labels.

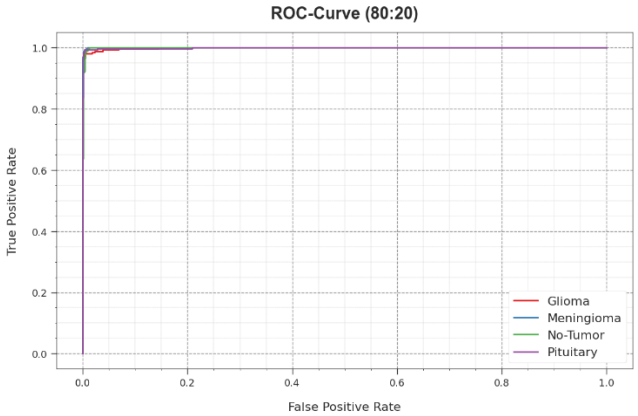

Figure 10: ROC curve of BTDC-OOADL method at 80%:20% of TRAS/TESS

A comparative outcome of the BTDC-OOADL technique with existing approaches was carried out is shown in Table 4 and Fig. 11 [24, 25, 26]. The simulated values indicate that the new 3DCNN and VGG19 approaches have shown the least outcomes. Along with that, the Inceptionv3, fine-tuned VGG-19, new 2D-CNN, and 3D-CNN systems obtained considerable performance. Although the ELCAD-BTC model has reached near-optimal performance, the BTDC-OOADL algorithm has shown maximum performance with maximum $accu_y$, $prec_n$, $reca_l$, and F_{score} values of 99.39%, 98.80%, 98.77%, and 98.78%, respectively. These experimental value shows that the BTDC-OOADL method exhibits superior performance over other models.

Table 4: Comparative outcome of BTDC-OOADL methodology with existing models

Methods	$Accu_y$	$Prec_n$	$Reca_l$	F_{score}
BTDC-OOADL	99.39	98.80	98.77	98.78
ELCAD-BTC	99.24	97.93	97.92	97.83
Novel 2D-CNN	98.00	97.14	96.99	97.08
Novel 3D-CNN	89.50	96.04	96.63	97.88
VGG-19 Model	90.70	97.73	97.45	96.89
Inception-V3	95.60	96.53	97.25	97.10
3D-CNN Model	98.32	97.49	96.32	96.57
Fine-tuned VGG-19	94.00	97.48	96.49	97.61

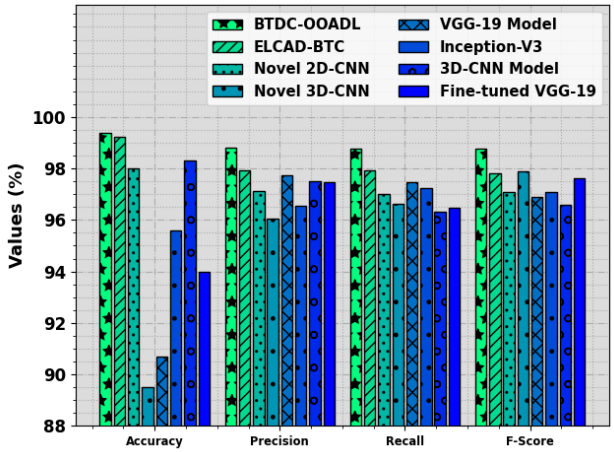

Figure 11: Comparative outcomes of BTDC-OOADL model with existing techniques

5. Conclusion

In this paper, we have introduced a new BTDC-OOADL for accurate classification and recognition of the BT on MRI Images. The BTDC-OOADL technique deeply investigates the MRI for the BT recognition. In the proposed BTDC-OOADL method, several subprocesses are included namely WF-based removal of noise, MobileNetv2 feature extractor, OOA-based parameter tuning, and GCN-based classification. Moreover, the BTDC-OOADL methodology can utilise the MobileNetv2 technique for the procedure of feature extractor. In the meantime, the OOA has been deployed for the boost parameter choice of the MobileNetv2 algorithm. Lastly, the GCN method can be utilized for the classification and recognition of BT. The experimental study of the BTDC-OOADL method was tested under benchmark databases. The simulation outcomes infer the better outcome of the BTDC-OOADL technique with recent approaches.

Funding: "This research received no external funding"

Conflicts of Interest: "The authors declare no conflict of interest."

References

[1] Kalyani, B.J.D., Meena, K., Murali, E., Jayakumar, L. and Saravanan, D., 2023. Analysis of MRI brain tumor images using deep learning techniques. Soft Computing, pp.1-8.

[2] Hashemzehi, R., Mahdavi, S.J.S., Kheirabadi, M. and Kamel, S.R., 2020. Detection of brain tumors from MRI images base on deep learning using hybrid model CNN and NADE. biocybernetics and biomedical engineering, 40(3), pp.1225-1232.

[3] Rammurthy, D. and Mahesh, P.K., 2022. Whale Harris hawks optimization based deep learning classifier for brain tumor detection using MRI images. Journal of King Saud University-Computer and Information Sciences, 34(6), pp.3259-3272.

[4] Abdusalomov, A.B., Mukhiddinov, M. and Whangbo, T.K., 2023. Brain Tumor Detection Based on Deep Learning Approaches and Magnetic Resonance Imaging. Cancers, 15(16), p.4172.

[5] Siddique, M.A.B., Sakib, S., Khan, M.M.R., Tanzeem, A.K., Chowdhury, M. and Yasmin, N., 2020, October. Deep convolutional neural networks model-based brain tumor detection in brain MRI images. In 2020 Fourth International Conference on I-SMAC (IoT in Social, Mobile, Analytics and Cloud)(I-SMAC) (pp. 909-914). IEEE.

[6] Ali, S., Li, J., Pei, Y., Khurram, R., Rehman, K.U. and Mahmood, T., 2022. A comprehensive survey on brain tumor diagnosis using deep learning and emerging hybrid techniques with multi-modal MR image. Archives of computational methods in engineering, 29(7), pp.4871-4896.

[7] Chattopadhyay, A. and Maitra, M., 2022. MRI-based brain tumour image detection using CNN based deep learning method. Neuroscience informatics, 2(4), p.100060.

[8] Rajendran, S., Rajagopal, S.K., Thanarajan, T., Shankar, K., Kumar, S., Alsubaie, N., Ishak, M.K. and Mostafa, S.M., 2023. Automated Segmentation of Brain Tumor MRI Images using Deep Learning. IEEE Access.

[9] Grampurohit, S., Shalavadi, V., Dhotargavi, V.R., Kudari, M. and Jolad, S., 2020, October. Brain tumor detection using deep learning models. In 2020 IEEE India Council International Subsections Conference (INDISCON) (pp. 129-134). IEEE.

[10] Lamrani, D., Cherradi, B., El Gannour, O., Bouqentar, M.A. and Bahatti, L., 2022. Brain tumor detection using mri images and convolutional neural network. International Journal of Advanced Computer Science and Applications, 13(7).

[11] Khan, M.A., Khan, A., Alhaisoni, M., Alqahtani, A., Alsubai, S., Alharbi, M., Malik, N.A. and Damaševičius, R., 2023. Multimodal brain tumor detection and classification using deep saliency map and improved dragonfly optimization algorithm. International Journal of Imaging Systems and Technology, 33(2), pp.572-587.

[12] Vankdothu, R. and Hameed, M.A., 2022. Brain tumor MRI images identification and classification based on the recurrent convolutional neural network. Measurement: Sensors, 24, p.100412.

[13] Haq, E.U., Jianjun, H., Li, K., Haq, H.U. and Zhang, T., 2021. An MRI-based deep learning approach for efficient classification of brain tumors. Journal of Ambient Intelligence and Humanized Computing, pp.1-22.

[14] Devanathan, B. and Kamarasan, M., 2023. Multi-objective Archimedes Optimization Algorithm with Fusion-based Deep Learning model for brain tumor diagnosis and classification. Multimedia Tools and Applications, 82(11), pp.16985-17007.

[15] Mandle, A.K., Sahu, S.P. and Gupta, G.P., 2022. CNN-based deep learning technique for the brain tumor identification and classification in MRI images. International Journal of Software Science and Computational Intelligence (IJSSCI), 14(1), pp.1-20.

[16] Aziz, A., Attique, M., Tariq, U., Nam, Y., Nazir, M., Jeong, C.W., Mostafa, R.R. and Sakr, R.H., 2021. An Ensemble of Optimal Deep Learning Features for Brain Tumor Classification. Computers, Materials & Continua, 69(2).
[17] Satyanarayana, G., Naidu, P.A., Desanamukula, V.S. and Rao, B.C., 2023. A mass correlation based deep learning approach using deep Convolutional neural network to classify the brain tumor. Biomedical Signal Processing and Control, 81, p.104395.
[18] Raza, A., Ayub, H., Khan, J.A., Ahmad, I., S. Salama, A., Daradkeh, Y.I., Javeed, D., Ur Rehman, A. and Hamam, H., 2022. A hybrid deep learning-based approach for brain tumor classification. Electronics, 11(7), p.1146.
[19] dos Santos, J.C.M., Carrijo, G.A., de Fátima dos Santos Cardoso, C., Ferreira, J.C., Sousa, P.M. and Patrocínio, A.C., 2020. Fundus image quality enhancement for blood vessel detection via a neural network using CLAHE and Wiener filter. Research on Biomedical Engineering, 36, pp.107-119.
[20] Indraswari, R., Rokhana, R. and Herulambang, W., 2022. Melanoma image classification based on MobileNetV2 network. Procedia computer science, 197, pp.198-207.
[21] Ismaeel, A.A., Houssein, E.H., Khafaga, D.S., Abdullah Aldakheel, E., AbdElrazek, A.S. and Said, M., 2023. Performance of Osprey Optimization Algorithm for Solving Economic Load Dispatch Problem. Mathematics, 11(19), p.4107.
[22] Miele, E.S., Bonacina, F. and Corsini, A., 2022. Deep anomaly detection in horizontal axis wind turbines using graph convolutional autoencoders for multivariate time series. Energy and AI, 8, p.100145.
[23] https://www.kaggle.com/datasets/masoudnickparvar/brain-tumor-mri-dataset
[24] Vaiyapuri, T., Jaiganesh, M., Ahmad, S., Abdeljaber, H.A., Yang, E. and Jeong, S.Y., 2023. Ensemble Learning Driven Computer-Aided Diagnosis Model for Brain Tumor Classification on Magnetic Resonance Imaging. IEEE Access
[25] T. Vivekanandan, J. Jegan, D. Jagadeesan, Y. Sreeraman, N. Ch. S. N. Iyengar, E. Purushotham. (2024). Internet of Things Enabled Based Arrhythmia Classification using Dandelion Optimization Algorithm with Ensemble Learning. Journal of Journal of Intelligent Systems and Internet of Things, 11 (2), 63-74 (Doi : https://doi.org/10.54216/JISIoT.110206)
[26] R. Rajkumar, Dınesh Valluru, Siva Satya Sreedhar P. , N. Ramshankar, Sujatha S. , Somasundaram R., M. Sudha, S. Navaneethan. (2024). Enhanced Jaya Optimization Algorithm with Deep Learning Assisted Oral Cancer Diagnosis on IoT Healthcare Systems. Journal of Journal of Intelligent Systems and Internet of Things, 11 (2), 97-110 (Doi : https://doi.org/10.54216/JISIoT.110209)